

# Grain Based Modeling of Stress Induced Copper Migration for 3D-IC Interwafer Vias

D.N. Bentz, M.O. Bloomfield, H. Huang, J.-Q Lu, R. J. Gutmann, and T.S. Cale

Focus Center- New York, Rensselaer: Interconnects for Gigascale Integration, Rensselaer Polytechnic Institute  
Troy, NY, USA, 12180-3590  
calet@rpi.edu

**Abstract**—We discuss our grain-continuum approach to modeling stress-driven grain boundary migration in polycrystalline Cu films, assuming that migration is due to differences in strain energies. We focus on thermally induced stresses and compute those using Comsol Multiphysics. To account for grain structure in polycrystalline films, the anisotropic elastic constants of single crystal Cu are used for each grain, after aligning them with each grain's orientation. Local grain boundary velocities are calculated based on the differences in strain energy across grain boundaries. The computed velocities are then used to update the level sets that represent the grain boundaries using the PLENTE software. Simple and more complicated grain structures are studied as part of a larger effort to understand the effects of thermally induced stresses in 3D-IC inter-wafer vias.

**Keywords**- Grain-continuum, grain boundary migration, thermal mechanical stresses, PLENTE

## I. MOTIVATION

We discuss our on-going thermo-mechanical modeling effort to provide parameters for the design and fabrication of 3D-ICs based on benzocyclobutene (BCB) wafer bonding [1]. Broadly speaking, the stability concerns for inter-wafer interconnect structures are extensions of those for MLM structures. One major reliability concern is the stability of the Cu vias that pass through several materials and layers.

We use the finite element package Comsol Multiphysics (CM) [2] for thermo-mechanical modeling of inter-wafer Cu vias. In [3] and [4], Cu was treated as a homogenous and isotropic material placed under stress from CTE mismatches with surrounding materials in structures such as the one displayed in Fig. 1a. The impact of grain structure on these systems was introduced via a Hall-Petch correlation of the Cu yield stress with grain size. We validated our approach by comparing our results to data from reliability studies of Cu via structures in SiCOH and SiLK [5,6], as well as XRD studies of Damascene-patterned Cu lines [7]. We concluded that the inter-wafer vias are susceptible to failure, depending on the BCB thickness, via pitch, and via diameter. Since these results indicate that stresses are a potential reliability issue, we are extending our model in order to improve our predictions of allowable design parameters and to examine the types of potential failures.

Because some dimensions of the structures in question are on the same length scale as the grains within the Cu, the granular nature of the Cu may significantly affect the

mechanical responses of the system [8]. As a first step we introduce idealized Cu grain structures into the mechanical models. Fig. 1a, 1b, and 1c compare thermally induced stress results using homogenous, 'single crystal', and polycrystalline structures. The materials properties used are reported in [2], except for the single crystal Cu properties reported below. These vias consist of a square column of Cu, 2 by 2 by 25  $\mu\text{m}$ . The materials stack consists of two 10  $\mu\text{m}$  MLM layers, four 1  $\mu\text{m}$  oxide layers, a 10  $\mu\text{m}$  Si layer, and a 2  $\mu\text{m}$  BCB layer. The two single crystal orientations,  $\langle 100 \rangle$  and  $\langle 111 \rangle$  Cu aligned with the via axis (1b and 1c respectively), are chosen to provide extreme values of Young's modules along the length of the via. As would be expected, the homogenous Cu model has stresses that fall between those of the  $\langle 100 \rangle$  and  $\langle 111 \rangle$  oriented Cu vias. In Fig 1d the Cu via is divided into rectilinear grains, which are assigned orientations by rotating the elasticity matrix of each material. A greater range of stresses are seen in this case than in either of the single crystal vias, but the exact

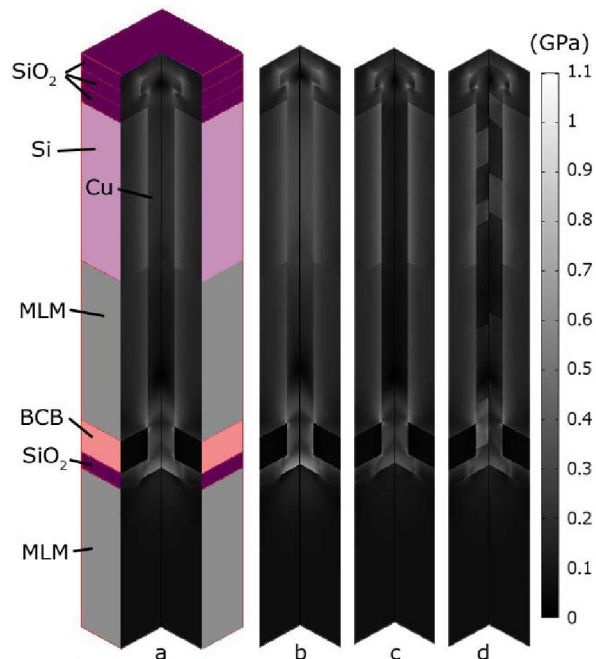


Figure 1. Von Mises stresses computed for a temperature change of 250  $^{\circ}\text{C}$  to 25  $^{\circ}\text{C}$  in representative 3D IC vias passing through a material stack. Properties of Cu used are: (a) isotropic bulk properties, (b) anisotropic properties associated with  $\langle 111 \rangle$  axes of Cu aligned with the via direction, (c) anisotropic properties associated with  $\langle 100 \rangle$  axes of Cu aligned with the via direction, and (d) an explicit grain structure ( $\sim 90$  grains) composed of 50%  $\langle 111 \rangle$  aligned and 50%  $\langle 100 \rangle$  aligned grains. In b, c, and d only the 'interiors' are shown.

range depends upon the orientation details. Extremes in stresses are most evident at the BCB layer, where the stresses in the Cu are the greatest. Moreover, the homogeneous isotropic results show large gradients in the stresses, which may provide driving forces for grain structure evolution. Since both the mechanical and electrical properties can be affected by grain structures, it is important to understand how they evolve in time.

The next step to improve the model is to consider the evolution of the structure due to the induced stresses. We have developed a modeling approach and a related software environment that allows us to study the evolution of 3D grain structures. Grain continuum (GC) models [9,10] treat grain structures as collections of individual continua that may interact but are distinct from each other. Each grain in a GC model is described by its location, boundaries, and any internal field variables, such as composition, stress, or temperature. We have reported on PLENTE [9-12], as a GC-based software that uses a multiple materials level set method to represent grains as continua as well as evolve grain structures in response to computed grain boundary velocities.

This paper discusses stress-induced grain boundary migration. As a base from which to proceed, we first discuss the elastic response of an idealized polycrystalline thin film constructed in CM. The model accounts for grain structure, including the orientations of the individual grains and their mechanical anisotropy. Using this simple GC model we compute the strain energy distribution. Grain boundary velocities are calculated from strain energy differences across grain boundaries (and mobilities). The structure and the velocities are exported into PLENTE where the structure is evolved. We then show a polycrystalline line segment developed in PLENTE and exported into CM. CM assigns mechanical properties and computes thermally induced strains and stresses in the line structure. The grain boundary velocities, which depend on the stresses, are computed and returned to PLENTE where the level set representations are updated.

## II. EFFECTS OF ELASTIC ANISOTROPY

Single grains of Cu have anisotropic elastic characteristics which impact the stresses in polycrystalline structures. The elastic modulus for single crystal Cu, as displayed in Fig. 2, is 2.9 times as large in the  $\langle 111 \rangle$  direction and 2.0 times as large in the  $\langle 110 \rangle$  than it is in the  $\langle 100 \rangle$  direction [13,14]. When a mechanical load is placed on a polycrystalline structure in which grains of different orientations are present, stresses are distributed throughout the grain structure in a complex manner [15,16].

In the finite element model, the elastic constants are assigned to each grain in the system through the elasticity matrix  $C_{grain}$ , which is defined as

$$\sigma = C_{grain} \epsilon_{el} \quad (1)$$

Here, the elasticity matrix relates the six components of the stress vector ( $\sigma$ ), including normal and shear components, to the strain in vector form ( $\epsilon_{el}$ ). The values in  $C_{grain}$  depend on the crystallographic orientation chosen for the particular grain. For

a crystal of Cu with the  $\langle 100 \rangle$  directions aligned with the lab frame, the elasticity matrix has three unique non-zero components;  $C_{11} = 168.4$  GPa,  $C_{12} = 121.4$  GPa, and  $C_{44} = 75.4$  GPa [14]. Once the desired orientation of a grain is chosen, the elasticity matrix is rotated [13,17].

In these elasticity models, grains are treated as individual elastic materials that undergo no topological changes during the stress-strain calculation. We also assume no slip occurs at grain boundaries or material interfaces. As an example, we examine an idealized thin film composed of hexagonally shaped Cu grains, as shown in Fig. 3a. The sample of film shown is a 6 by 5.2  $\mu\text{m}$  rectangle containing 17 grains (or parts of grains). The 1  $\mu\text{m}$  thick film has been deposited on an oxidized 1 mm thick silicon wafer where the oxide layer is 1  $\mu\text{m}$  thick. The geometry is periodic in the plane, and is not capped. The system is cooled from an assumed stress-free state at 525 K to 425 K and the stresses from the CTE mismatch between the various materials are computed. When the Cu film is treated as homogeneous and isotropic using the properties of bulk Cu (the grains are ignored), it exhibits a uniform strain energy value throughout the Cu of  $\sim 0.4$  J/cm<sup>3</sup>. When the film consists of grains with their  $\langle 111 \rangle$  axes perpendicular to the film surface, the strain energy [18] resulting from the temperature change is  $\sim 0.6$  J/cm<sup>3</sup> MPa. It is 50% higher than the isotropic case due to the larger in-plane Young's modulus.

Fig. 3a shows the strain energy distribution computed for a similar film in which one of the grains has been rotated such that a  $\langle 100 \rangle$  axis is aligned with the surface normal. Inside and around the  $\langle 100 \rangle$  grain the strain energy density range from  $\sim 0.9$  J/cm<sup>3</sup> to  $\sim 0.4$  J/cm<sup>3</sup>. The effective Young's modulus of the center grain in the plane of the film is significantly lower than the moduli of the grains around it. This effect illustrates how grain structure can provide a driving force for migration of atoms, dislocations, or vacancies.

## III. STRESS-INDUCED GRAIN BOUNDARY MOTION

Models that include strain energy as a driving force for grain boundary motion have been used, together with curvature driven grain boundary migration [19] to explain the influence of strain on abnormal grain growth in Cu films [20,21]. We write the effect of strain energy difference across a grain boundary,  $\Delta u$ , on the grain boundary velocity as proportional to

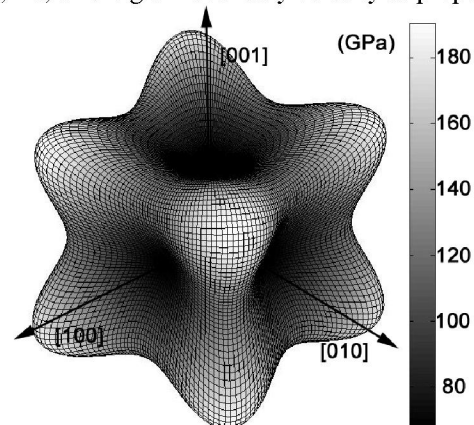


Figure 2. Spherical plot of the directional dependence of Young's modulus for single crystal Cu.

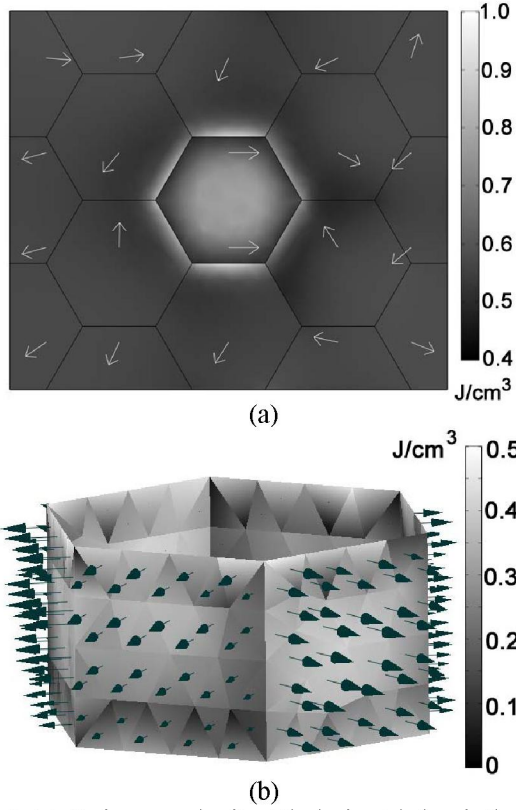


Figure 3. (a) Strain energy density at the horizontal plane in the middle of the film. Grains are oriented with their  $\langle 111 \rangle$  axis normal to the plane of the film and a uniform, random distribution of in-plane rotations, except for the center grain which is rotated such that the  $\langle 100 \rangle$  axis is aligned with the normal to the plane of the film. Arrows represent the projections of the  $\langle 100 \rangle$  directions. (b) Arrows show the magnitude and direction of the computed grain boundary velocities, as computed using the differences in strain energies between the  $\langle 100 \rangle$  and  $\langle 111 \rangle$  grains.

the grain boundary mobility  $M_{GB}$  [19].

$$\mathbf{v}_g = \Delta u M_{GB} \hat{\mathbf{n}}_{GB} \quad (2)$$

Here  $\hat{\mathbf{n}}_{GB}$  is a unit vector normal to the grain boundary pointing towards areas of higher strain energy. As atoms leave a grain of high strain energy and move across a grain boundary to a grain with lower strain energy, the grain boundary moves in the opposite direction. Strain energy is computed in terms of the components of stress  $\sigma_i$  and strain  $\epsilon_i$ .

$$u = \frac{1}{2} \sum_i \epsilon_i \sigma_i \quad (3)$$

The mobility may be expressed as

$$M_{GB} = \frac{b v \Omega}{kT} \exp\left(-\frac{\Delta G}{kT}\right) \quad (4)$$

Here  $b$  is the distance the grain boundary is displaced by the addition of an atom,  $v$  is the Debye frequency,  $\Omega$  is the atomic

volume,  $k$  is the Boltzmann constant,  $T$  is absolute temperature and  $\Delta G$  is the free energy associated with atomic exchange across the grain boundary [12,22].

To illustrate, we examine the grain boundary motion for the computed strain energies of the Cu film shown in Fig. 3. Using the same stress conditions as described above, where the internal stresses are generated by lowering the temperature 100 K from a stress free state of 525 K, we examine the strain energy distribution of the film composed of a  $\langle 100 \rangle$  textured grain surrounded by grains of  $\langle 111 \rangle$  texture. This structure exhibits strain energy differences between the  $\langle 100 \rangle$  and  $\langle 111 \rangle$  grains of 0.1 to 0.45 J/cm<sup>3</sup>. Using literature values for the terms of  $M_{GB}$  [23,24] and approximating  $\Delta G$  as 1 eV [12,22], we see that stresses in the film promote the growth of the  $\langle 100 \rangle$  grain. While the center of the  $\langle 100 \rangle$  grain has higher strain energies than the surrounding  $\langle 111 \rangle$  grains, at the grain boundary the  $\langle 100 \rangle$  strain energies are lower. This is attributed to the  $\langle 100 \rangle$  grain being softer in the plane of the film and strain in the plane of the grain boundary being continuous due to the no-slip condition. This result is consistent with simulations of 2D films [19] and with experimental studies [20].

To see the effect of grain boundary velocities on grain structure, the velocities are exported into PLENTE, as normal speeds on the triangles that represent the grain boundaries. PLENTE evolves the grain structure, based on the imported velocities, as seen in Fig 4. The fastest-moving grain boundaries in the system are those along the  $\langle 100 \rangle$  grain. Although the shape of the grain structure has two bilateral symmetries, the anisotropy of the grain orientations breaks that symmetry, and the evolution is asymmetric. Fig. 4 shows the result of one Euler time integration (constant strain energies for the time step). Cycling between CM and PLENTE provides large grain evolutions, as seen for curvature driven evolution during annealing after electrochemical deposition of Cu [10,12]

#### IV. GRAIN BOUNDARY MIGRATION IN A CU LINE

We demonstrate the interaction of PLENTE and CM using a segment of a polycrystalline Cu line completely encapsulated in an oxide layer on a silicon wafer. Fig. 5a shows the initial structure developed in PLENTE using an isotropic deposition model. A grain boundary-fitted finite element mesh was developed by PLENTE, as an extension of the method detailed in [25], and exported to CM. In CM, all grains in the line,

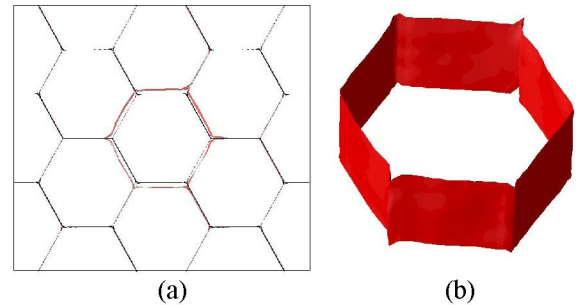


Figure 4. (a) Top view of the level set grain boundaries in PLENTE before (in black) and after 12.5 hours at 425K (in red). (b) Perspective image of the grain boundary of the center grain evolved using PLENTE.

except for one, have a  $\langle 111 \rangle$  orientation with respect to the surface of the line. The front/center grain in Fig. 5 has a  $\langle 100 \rangle$  orientation. We use these particular grain orientations only to illustrate the model. Stresses are generated in the line structure by cooling it from a stress free-state at 525 K down to 425 K. For this temperature change, strain energies in the line are between 0.1 and 0.4 J/cm<sup>3</sup>. Strain energy differences between the  $\langle 100 \rangle$  and  $\langle 111 \rangle$  grains are between 0.0 and 0.2 J/cm<sup>3</sup>. Grain boundary velocities are computed as discussed above and are exported back into PLENTE where the level-set representation is updated. Fig. 5b shows one view of the line segment after evolving the structure for 30 hours. The motions of the grain boundaries are clear, but interpreting them is more complex than in the thin simple film studied above. The  $\langle 100 \rangle$  grain is surrounded on three sides by grains of  $\langle 111 \rangle$  texture as well as the oxide. There is a need to develop better methods to represent and summarize the results of 3D structural evolutions, such as the ones presented here.

## V. CONCLUSIONS

We present an approach to using grain-continuum models to examine the effects of thermally induced stresses on grain evolution. Thermo-mechanical modeling of 3D-ICs indicates that grain structure can be important in predicting the reliability of these structures. We see that the range of von Mises stresses is greater than the stresses calculated from using the uniform properties of the constituent grains. Finite element calculations indicate that differences in strain energy can be high in polycrystalline films. The model we present uses the strain energy difference between grains as driving forces for grain boundary evolution. These differences are converted to grain boundary velocities using estimates of grain boundary mobilities. A level-set based code, PLENTE, uses these velocities to evolve a level-set representation of the system. The cycle can be repeated to achieve large changes in grain structure. CM and PLENTE interact by exchanging grain-boundary fitted meshes. The evolution of grains may not be limited to the interaction between grains, but influenced by the elastic properties of the surrounding materials. It is expected that, in systems such as 3D-ICs, that the stiffness of each material will affect the strain energy distribution. This approach forms the basis for simulations of evolution in Cu inter-wafer vias used in 3D-ICs, in addition to many other applications both inside and outside of microelectronics.

## ACKNOWLEDGMENTS

This work was supported by MARCO, DARPA and NYSTAR through the Interconnect Focus Center.

## REFERENCES

- [1] J.-Q. Lu, *et al.*, in *Proc of 2002 IITC*, 2002 (IEEE), p. 78-80.
- [2] Comsol Multiphysics 3.2, Comsol, Inc. <http://www.comsol.com>.
- [3] J. Zhang, M. O. Bloomfield, J.-Q. Lu, R. J. Gutmann, and T. S. Cale, *Microelec. Eng.* **82**, 534 (2005).
- [4] D. N. Bentz, *et al.*, in *Proc. 22nd VMIC, IMIC*, 2005, p. 89.
- [5] D. Edelstein, *et al.*, in *Proc. 2004 IRPS*, 2004 (IEEE), p. 316-19.
- [6] R. G. Filippi, *et al.*, in *Proc. 2004 IRPS*, 2004 (IEEE), p. 61-7.
- [7] S.-H. Rhee, Y. Du, and P. S. Ho, *J. Appl. Phys.* **93**(7), 3926 (2003).

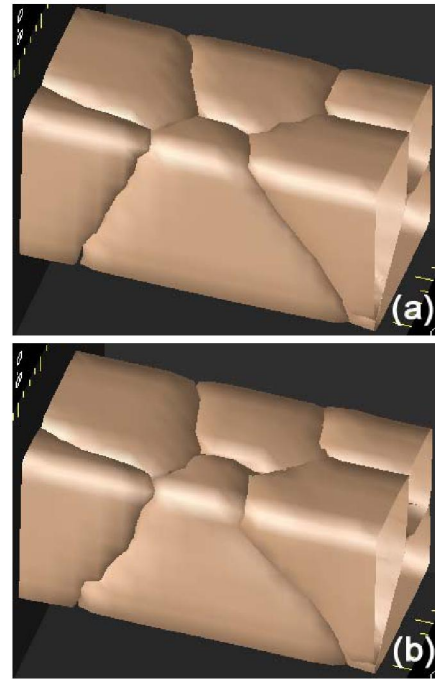


Figure 5. (a) Initial grain structure in an encapsulated line of 0.4 by 0.4  $\mu\text{m}$  cross section, obtained from an electrochemical deposition simulation. Surrounding oxide is not displayed. (b) Grain structure after 30 hours of evolution with the strain energy driven model. For demonstration purposes, time evolution is carried beyond the likely range

- [8] M. Nygard, *Mech. Mat.* **35**(11), 1049 (2003).
- [9] T. S. Cale, M. O. Bloomfield, D. F. Richards, K. E. Jansen, and M. K. Gobbert, *Comp. Mat. Sci.* **23**(1-4), 3-14 (2002).
- [10] M. O. Bloomfield, Y. H. Im, and T. S. Cale, in *Proc. 2003 SISPAD*, 2003 (IEEE), p. 19-22.
- [11] M. O. Bloomfield, D. F. Richards, and T. S. Cale, *Phil. Mag.* **83**(31-34), 3549-68 (2003).
- [12] M. O. Bloomfield and T. S. Cale, *Microelec. Eng.* **76**, 195-204 (2004).
- [13] S. G. Lekhnitskii, *Theory of elasticity of an anisotropic body* (Mir Publishers, Moscow, 1981).
- [14] G. Simmons and H. Wang, *Single crystal elastic constants and calculated aggregate properties: a handbook* (M.I.T. Press, Cambridge, MA, 1971).
- [15] S. P. Baker, A. Kretschmann, and E. Arzt, *Acta Mat.* **49**(12), 2145 (2001).
- [16] P. Gudmundson and A. Wikstrom, in *Proc. 2002 MAM*, 2002, p. 17-29.
- [17] A. F. Bower, "Lecture notes: EN175:" *Advanced Mechanics of Solids*, Brown University, <http://www.engin.brown.edu/courses/en175>, (2005).
- [18] W. F. Hosford, *Mechanical Behavior of Materials* (Cambridge University Press, New York, 2005).
- [19] R. Carel, C. V. Thompson, and H. J. Frost, *Acta Mat.* **44**(6), 2479-94 (1996).
- [20] E. M. Zielinski, R. P. Vinci, and J. C. Bravman, *Appl. Phys. Lett.* **67**(8), 1078-80 (1995).
- [21] C. V. Thompson, *Ann. Rev. Mat. Sci.* **30**, 159-190 (2000).
- [22] M. Upmanyu, R. W. Smith, and D. J. Srolovitz, *Interface Sci.* **6**, 41-58 (1998).
- [23] C. Kittel, *Introduction to Solid State Physics 6th ed.* (John Wiley and Sons, Inc., New York, 1986).
- [24] *CRC Handbook of Chemistry and Physics*, edited by R. C. Weast (CRC Press Inc, Boca Raton, FL, 1983).
- [25] M.O. Bloomfield, D.F. Richards, and T.S. Cale, *Lecture Notes in Comp. Sci.* **3516**, 49-56 (2005).